Published in final edited form as:
Cancer Res. 2011 June 1; 71(11): 3872–3880. doi:10.1158/0008-5472.CAN-10-4482.

Mild elevation of body temperature reduces tumor interstitial fluid pressure and hypoxia, and enhances efficacy of radiotherapy in murine tumor models

Arindam Sen, **Maegan L. Capitano**, **Joseph A. Spernyak**[*], **John T. Schueckler**, **Seneca Thomas**, **Anurag K. Singh**[†], **Sharon S. Evans**, **Bonnie L. Hylander**, and **Elizabeth A. Repasky**
Department of Immunology, Roswell Park Cancer Institute Buffalo, New York

[*]Department of Animal Resources Roswell Park Cancer Institute Buffalo, New York

[†]Department of Radiation Oncology Roswell Park Cancer Institute Buffalo, New York

Abstract

Patient and rodent solid tumors often exhibit elevated interstitial fluid pressure (IFP). This condition is recognized as a prognostic indicator for reduced responses to therapy and decreased disease-free survival. Here we tested whether induction of a thermoregulatory-mediated rise in tissue blood flow, induced by exposure of mice to mild environmental heat stress, could influence IFP and other vascular parameters within tumors. Using several murine tumor models, we found that heating results in a *sustained reduction* in tumor IFP correlating with increased tumor vascular perfusion (measured by fluorescent imaging of perfused vessels, laser Doppler and magnetic resonance imaging) as well as a sustained reduction in tumor hypoxia. When radiation therapy was administered 24 hours post-heating, we also observed a significant improvement in efficacy that may be a result of the sustained reduction in tumor hypoxia. These data suggest, for the first time, that environmental manipulation of normal vasomotor function is capable of achieving therapeutically beneficial changes in IFP and microvascular function in the tumor microenvironment.

Keywords

Tumor microcirculation and microenvironment; Noninvasive imaging in animal models; Modification of radiation sensitivity; Hyperthermia; Hypoxia; Interstitial fluid pressure Thermoregulation

INTRODUCTION

Tumor blood vessels often lack adequate smooth muscle coverage and exhibit both defective vasomotor activity and increased permeability (1–3). This creates a microenvironment in which fluid accumulation and increased protein concentration (resulting in increased oncotic pressure (4)) contributes significantly to elevated interstitial fluid pressure (IFP) (5, 6). The degree of elevation differs both between tumors and regionally within tumors. Patient tumors and human tumor xenografts exhibit IFPs ranging from a low of 2.6 mmHg to a high of 40 mmHg, in contrast to the IFP of normal tissue which is typically −3 to +3 mmHg (5,

Address Correspondence to: Elizabeth A. Repasky, Ph.D. Dept of Immunology Roswell Park Cancer Institute Buffalo, New York 14263 Phone: 716-845-3133 Fax: 716-845-8552 elizabeth.repasky@roswellpark.org.

7–9). While there are fewer studies on IFP measurements in murine tumor models, those reported are also elevated, ranging from 3.6 to 15 mmHg (10–12).

That elevated IFP could impede delivery of therapeutics into tumors was recognized two decades ago (13) and currently the challenge of delivering therapeutic drugs and antibodies into the interior of tumors is clearly recognized (5, 9, 14). Interestingly, cytotoxic drugs (diphtheria toxin (15), taxanes (10) and paclitaxel (16)) which kill tumor cells directly, may "decompress" tumors leading to improved tumor vascular function as well as decreased tumor IFP (10, 16). Consistent with these observations is a recent report demonstrating that following chemotherapy, early decrease in IFP was predictive of a better tumor response (12). Elevated IFP also compromises the response of tumors to radiotherapy (3, 17). Since hypoxia is clearly related to radioresistance, it has been suggested that the abnormal vascularization of tumors leads to increased hypoxia whereas reperfusion could improve radiosensitivity of tumors (18) Recently, it was reported that in a head and neck xenograft model, treatment with the EGFR inhibitor erlotinib led to decreased HIF-1α and VEGR expression, which in turn led to vascular normalization, improved blood flow, increased oxygenation and improved response to radiotherapy (19). However, whether IFP was altered by erlotinib was not measured in this study. Importantly, *pretreatment IFP* has also been shown to be an independent prognostic factor for the survival of patients with cervical cancer treated with radiotherapy (8). Further, using a human melanoma xenograft model, it was determined that while IFP was variable within a cohort of tumors, tumors with lower IFP had better response to subsequent radiotherapy (20). These data relating lower IFP with improved response to radiotherapy supports the need to identify strategies that *can safely reduce tumor IFP*.

Cancer researchers have long been interested in the radio-sensitizing effects obtained by local delivery of heat to tumors, with the goal of achieving cytotoxic temperatures between 42–45°C (21–23), a range which can kill tumor cells as well as vascular endothelium. However, other research has revealed that local heat treatments at milder temperatures between 39 and 42 °C can improve oxygenation of tumors and vascular perfusion, and also result in radiosensitization (reviewed in (24–27)). Work by others (28, 29) and ourselves (30) has shown positive anti-tumor effects of using mild systemic heating at physiologically achievable temperatures (39 – 39.5°C). Here, both normal and tumor tissue are heated, raising the possibility (31) that homeostatic, thermoregulatory mechanisms designed to control core body temperature could be engaged (31, 32) Since our initial studies revealed that the microvasculature of experimental murine tumors (but not normal organs) exhibited evidence of improved perfusion which persisted well beyond the period of heating of the mice, (30, 33), we decided to explore whether these thermally induced vascular changes could affect tumor IFP. Using three murine models, we found that mild systemic heating significantly reduced tumor IFP and that this effect was sustained for at least 24 hours post-heating. Importantly, this effect correlated with increased vascular perfusion, a reduction in tumor hypoxia and a significant improvement in response to radiotherapy. Collectively, our data support the hypothesis that targeting normal, thermoregulatory vasomotor function results in therapeutically beneficial changes in the tumor microenvironment.

Materials and Methods

Animal models

The murine colon tumor 26 (CT26) in BALB/c mice and murine melanoma B16.F10 in C57BL/6 mice were grown by subcutaneous injection of 1×10^6 cells; murine mammary 4T1 tumors by injection of 1×10^6 cells in the mammary fat pads of female BALB/c mice. Tumor volume was determined using the formula, volume = width^2 × length/2. Animal studies were approved by RPCI's Animal Care and Use Committee. Mice were obtained from the

National Cancer Institute. All cell lines were obtained from the American Type Culture Collection (ATCC).

Whole body heating

Body temperature of mice was raised using an environmental chamber (Memmert Model BE500, East Troy, WI), as previously published (30). Sentinel mice (one per cage) were implanted with temperature transponders subcutaneously near the shoulder (BioMedic Data Systems, Inc. Seaford, DE) two days prior to heating. The transponder reading ("body temperature") is typically within ±0.1°C of the core temperature measured by rectal probe (33). Mice were injected with 1 ml sterile saline, intraperitoneally, to prevent dehydration, and then placed in a cabinet at room temperature (22°C) or in pre-heated cages (38.5°C) in the incubator. Temperatures of sentinel mice were recorded initially every 30–45 minutes for the duration of the heating.

IFP measurement

Interstitial fluid pressure was measured by a modified "wick-in-needle" technique using custom designed instrumentation based upon a published design (11). Measurements were made with a MikroTip Catheter Transducer (Model SPR-524, Millar Instruments) via a 23.5 gauge wing-tipped needle. The transducer was interfaced to a PC using a pressure control unit (PCU-2000, Millar Instruments) via an USB analog-to-digital converter (Model DT9816 Data Translation, Marlboro MA). The software used to acquire the data was developed in our laboratory using DT Measure Foundry Ver. 4.0.7 (Data Translation, Marlboro, MA). The needle was inserted into the tumor and measurements were taken every few millimeters along the entry path and averaged. The instrument was calibrated using a custom built water-column manometer.

Detection of perfused blood vessels

To visualize perfused blood vessels, 50 μl of 0.4 mg/ml (in 75% DMSO) fluorescent dye $DiOC_7(3)$ (34) was administered via tail vein 2h after heating; 30s later, the animal was sacrificed. Tumors and muscle were resected, embedded in Tissue-Tek OCT and 6 – 10 μm sections cut. Images were recorded and DiOC7 profiles counted manually or using a particle analysis routine in NIH Image J. Total number of blood vessels were visualized using rat anti-mouse CD31 antibody (BD Pharmingin; clone MEC13.3).

Tumor blood flow measurements

Tumor blood flow by laser Doppler was measured using OxyFlo™ (Oxford Optronix Inc., Oxford, U.K.) fitted with a surface probe. Hair was removed 24h prior to measurements. Measurements were made in independent groups of unheated controls or in mice 2 h after heating by using probes at five different locations on the tumor surface. A series of five measurements at each site were recorded and averaged to determine blood flow in the tumor in Blood Perfusion Units (BPU).

Determination of fractional vascular volume by MRI using albumin-GdDTPA$_{35}$

Image acquisition—The change in fractional vascular volume (fVV) of intra-tumoral vessels in response to heating was monitored using contrast-enhanced MR imaging (35, 36). CT26 cells were implanted subcutaneously in the hind legs of BALB/c mice either unilaterally or bilaterally, and grown to a volume of 200–400 mm^3 before being imaged. These tumor volumes were used to ascertain adequate sampling of tumor associated voxels and to reduce possible artifacts from differences in magnetic susceptibilty between air and tumor tissue. A group of mice (10 tumors) underwent heating, were acclimated to room temperature for 1 hour and then imaged; unheated control mice (9 tumors) were not heated.

Imaging was performed on a 4.7 Tesla MRI system using a 35-mm transceiver coil (Bruker Biospin, Billerica, MA). Anesthesia was maintained during imaging with 2–3% isoflurane, and animal temperature and respiration were monitored and maintained using a physiologic monitoring system (Model 1025, SA Instruments, Stony Brook, NY). Following scout scans, three baseline R1 (1/T1 time) measurements were acquired using a fast spin-echo, saturation recovery method with variable repetition times (TR = 360 to 6000ms). Additional scan parameters were as follows: effective echo time = 20 ms, field-of-view = 32×32 mm, matrix size=128×96, slice thickness = 1mm, averages = 1, acquisition time=5 minutes. Following baseline R1 measurements, mice were injected via tail vein with albumin-$(GdDTPA)_{35}$ (Contrast Media Laboratory, USFC, California) at a concentration of 0.1 mmol/kg. A 3D angiography scan was acquired to confirm the quality of the injection, and then serial R1 measurements were obtained for up to 45 minutes post-injection.

Image analysis—Regions of interest (ROIs) for tumor and back muscle were drawn using commercially-available software (Analyze 7.0, AnalyzeDirect, Overland, KS). Average signal intensities at each TR were determined within each ROI and the R1 values were calculated by nonlinear fitting of the equation: $S_{(TR)} = S_{MAX} (1 - e^{-(R1 \cdot TR)})$ using Matlab (Matlab® 2008a, MathWorks Inc., Natick, MA). The increase in R1 (ΔR1), which is proportional to contrast agent concentration, was calculated by subtracting the average baseline R1 value from each post-injection value. To account for injection variability, ΔR1 values for the tumor were normalized by dividing the ΔR1 of the back muscle. Fractional vascular volumes of the tumors were obtained from the y-intercept of a linear regression fit of ΔR1 vs. time elapsed post-injection (37). A single data point in the control group was deemed an outlier by the extreme studentized deviate method ($p<0.05$) and excluded from statistical analysis. T1 relaxation rate parameter maps were calculated from the first T1 measurement acquired after contrast agent injection on a pixel-by-pixel basis. To determine the increase in R1, the pre-injection T1 rate of the tumor was subtracted from the generated R1 map. The ΔR1 maps were then normalized by dividing by the mean ΔR1 of back muscle. A color lookup table was applied to the ratio maps and overlaid upon black & white anatomic images.

Hypoxyprobe-1 administration and immunohistochemistry

Pimonidazole hydrochloride (60 mg/kg) was administered intraperitoneally at 2, 24 and 48h post-heating. Tumors were collected 45 minutes post-injection (following product insert from the manufacturer), fixed in 10% formalin and embedded in paraffin. Immunohistochemistry was performed on 6 – 10 μm paraffin sections according to the manufacturer's protocol (Hypoxyprobe-1 Plus Kit, Chemicon International HP2-100). Brightfield images were acquired using a Spot2 camera and Spot Advanced version 3.5.9.1 software (Diagnostic Instruments, Inc., Sterling Heights, MI).

Local radiation treatment

Animals were heated 24 hours prior to the first radiation treatment. CT26 tumor bearing mice received 4 Gy of radiation, fractionated over four days at 1Gy/day. B16.F10 tumor bearing mice received 20Gy fractionated over five days at 4Gy/day. Initial tumor volumes were 120 – 130 mm^3. For radiation treatment the mice were anesthetized with isofluorane (induction at 3–5%, maintenance at 1 – 2%). Mice were shielded with 2mm thick lead plates with small apertures limiting exposure to the tumors. Radiation was performed with an orthovoltage X-ray machine (Philips RT250, Philips Medical Systems) at 75 kV using a 1×2 cm cone. Experiments were ended when mice had to be removed from a group due to large tumor volume (~1500mm^3) or due to tumor ulceration.

Statistics

ANOVA with Dunnett's multiple comparison tests was used when comparing the means of multiple treatment groups to a control untreated group; Students' T-test was used when comparing the means of only two groups. Significant statistical differences between unheated control group and the treated groups are labeled as *, ** and *** for $p<0.05$, <0.01 and <0001 respectively.

Results

Tumor interstitial fluid pressure is reduced after heating

Mice bearing CT26 tumors (300–600mm^3) were heated to 39.5°C for 6h and then returned to room temperature (~21–22 °C); control mice were unheated. IFP measurements were performed at 2h post-heating. A third group received 2 doses of paclitaxel (30mg/kg; 48h apart), a treatment shown to reduce tumor IFP (16) and IFP was measured 24h after the second dose. We observed a significant reduction of tumor IFP in animals heated for 6h (1.27±0.49 vs. 3.37±0.45 cm H_2O in controls $P<0.05$), although there was a range in the IFP values of tumors within each group (Figure 1A) and this reduction was comparable to that resulting from paclitaxel treatment (1.6±0.24 cm H_2O). Similar results were obtained when mice bearing B16.F10 tumors were heated for 6h (Figure 1B; 5.93±0.6 in controls vs. 3.7±0.23 at 2h post heating and 2.83±0.34 cm H_2O at 24h post heating, $P<0.01$).

To determine both the kinetics and durability of IFP reduction, a time course study was conducted. Tumor bearing mice were heated to 39.5°C for 2, 4 and 6h. In CT26, a significant reduction in tumor IFP was achieved by 2h of heating (Figure 1C). Further we found that following a 6h heat treatment, the drop in IFP lasted for at least 24h (Figure 1C). In *orthotopically* implanted mammary 4T1 tumors, the effect of heating was comparable to that in the *subcutaneous* models Figure 1D). Collectively, the results demonstrate that a temporary increase in body temperature results in a significant reduction in tumor IFP which was observed to be maintained at 24h post heating in CT26 and B16.F10. The measured IFPs in the different murine tumors are all within the range of IFPs that have been reported in the literature for different tumors.

Tumor vascular perfusion increases after heating

To determine if heating (and reduced IFP) also alters vascular perfusion, we evaluated the effect of heating on distribution of a fluorescent dye within tumors vessels. Heated and unheated mice bearing CT26 tumors were injected with $DiOC_7(3)$ and the number of vessels perfused by the dye were counted. Overall a significant increase in perfused vessels was observed following heating although, again, there was a range of response. A visual comparison of representative sections (Fig. 2A) demonstrates that a tumor from a heated mouse has approximately twice the number of labeled vessels as a tumor from an unheated mouse (160 vs. 82). Interestingly, normal tissue (skeletal muscle) shows no difference in perfusion (Fig. 2A). Quantification of the vessels demonstrates that while there is a near doubling of $DiOC_7(3)$ perfused vessels in tumor sections from heated mice, there is no change in the number of CD31+ vessels in the same section (Figure 2B). This suggests that heating results in opening of a large fraction of previously unperfused vessels.

The reduction in IFP following heating correlates with an increase in blood flow

To test whether decreased IFP following heating correlates with increased tumor blood flow, both IFP and tumor blood flow were measured in an unheated control and a heated group of CT26 tumor bearing mice. For each tumor, blood flow (Doppler) measurements were performed first followed by IFP measurements. The results (Figure 3A and B) show that

decreased IFP is correlated with increased blood flow and these differences are statistically significant.

The increase in the number of perfused vessels and the increase in blood flow in tumors would be expected to result in an increase in the fractional vascular volume of tumors when determined using macromolecular contrast-enhanced MRI. Pseudo-colorized perfusion maps of CT26 tumors overlaid upon anatomical images from representative mice are shown in Figure 3C. The upper panels show perfusion maps from 4 control mice and the lower panels show perfusion maps of tumors from heated mice. The degree of perfusion is color coded such that red indicates greater perfusion. A 6-fold difference in the ratio of the fractional vascular volume (fVV) to muscle was observed in tumors of the heated group (n=10) versus the control group (n=8) (Figure 3D).

Hypoxia in tumors is reduced by heating

To determine whether increased blood flow in tumors following heating is associated with reduced hypoxia, we visualized changes in tumor hypoxia by immunohistochemical analysis of Hypoxyprobe localization. The severity of hypoxia present in sections of tumors from unheated and 2, 24 and 48h post-heating was scored (Fig. 3E). At 2h post-heating, the degree of hypoxia was greatly reduced compared to unheated tumors; there was some increase in hypoxia at 24h and 48h post-heating, (Figure 3F). This data indicates that heating results in a decrease in tumor hypoxia with the effect lasting for 24h post-treatment.

The efficacy of radiation therapy is enhanced by heating

We next asked whether the reduced IFP, increased vascular perfusion and decreased hypoxia observed following heating could improve efficacy of subsequent radiation treatment. To test this CT26 tumor bearing mice were divided into four groups (average size 120 – 130mm^3): 1) unheated control; 2) heating only (day 11); 3) fractionated radiation (1Gy per day for four days, days 12–15); and 4) 6h heating (39.5°C) followed 1 day later by fractionated radiation (Figure 4A). Heat treatment was given 24h before radiation based on previous findings (Fig. 1) that IFP levels are at their lowest at this time point and preliminary studies (data not shown) in which there was no indication of improvement if radiation was given on the same day as heating. Tumors in the unheated and heated only groups grew at a similar rate and were terminated on day 22 based on tumor size (volume >1,500 mm^3). The growth of tumors in mice receiving only radiation was moderately inhibited. However, growth of tumors in mice that were heated followed by radiation was significantly inhibited and this effect was maintained for the duration of the experiment.

Similar results were obtained with B16.F10 tumor-bearing mice. Again, mice were divided into four groups (average tumor size 100–150mm^3, n=5): 1) unheated control; 2) heating only (day 10); 3) fractionated radiation (4Gy/per day for 5 days, days 11–15); and 4) heating followed by fractionated radiation. .Again, tumors in the unheated and heated groups grew at the same rate (Figure 4B). While tumor growth in the group that received radiation only and the group treated by heating followed by radiation was inhibited, the growth of tumors in the combination treatment group was statistically significantly reduced compared to tumors treated with radiation alone beginning at day 22. Each of these experiments was repeated with similar outcomes (data not shown).

DISCUSSION

Thermoregulation is a long conserved homeostatic mechanism achieved by extensive local and central nervous system control of cardiovascular function, resulting in dynamically regulated vasodilation and vasoconstriction of blood vessels, and is essential for maintaining

core temperature when the system is faced with environmental or metabolic thermal stress (31, 32, 38, 39). Here we asked whether the tumor microenvironment is affected by triggering this normal response needed for optimal heat dissipation. We found that heating mice with tumors can *significantly reduce tumor IFP and hypoxia.* We also observed a significant improvement in the efficacy of radiation therapy administered 24 hours post-heating, an effect that may be a result of the sustained reduction in tumor hypoxia. While the specific cascade of vasomotor activity in normal tissues that leads to changes within the tumor microenvironment must still be identified, thermoregulatory-mediated increased blood flow in vascular beds proximal and distal to the tumor vasculature may help to, at least temporarily, improve blood flow through the tumor perhaps by drawing excess fluid from tumor stroma. This would in turn reduce IFP, decompress tumor vasculature and allow more blood to traverse the tumor.

While we found no sustained changes in blood flow in normal organs post-heating, which is the expected result of dynamic neurovascular control normally exerted over blood flow during thermoregulatory function, blood flow in tumors remained altered for an extended period of time. This suggests that among the abnormal properties of tumor vasculature, an apparent marked limitation in reversible vasomotor control when faced with a temporary challenge to the thermoregulatory system can be added to the list of defects. However, this defect in tumor vascular perfusion can be exploited to provide a window of time in which access to the tumor microenvironment may be enhanced without further increasing access to normal organs. This suggests that in addition to improving the efficacy of radiation therapy (as shown here in Fig. 4), mildly pre-heating animals may benefit other therapies which depend upon improved vascular access to tumors, including chemotherapy, nanoparticle and antibody therapies, and adoptive cellular immunotherapy. Indeed, in a previous study, we measured a significant increase in the uptake of liposomal doxorubicin following systemic hyperthermia (30) which resulted in improved tumor growth control. Such a strategy could be feasible in humans since an increase in core temperature by less than 1 degree C results in rapid, cutaneous vasodilation and movement of blood from the core to the skin for heat dissipation (31). It will next be important, using these murine pre-clinical models, to look at deeper seated tumors (e.g. kidney, liver or intestinal tract. Since heat-induced changes in vasomotor activity occur internally also (32, 38–40); it is likely that deeper tumors will also be significantly impacted by thermal signals. It will also be important to study endogenously-arising tumors since their vascular properties may be more similar to patient tumors than that of transplantable tumor models.

Since tumors are devoid of neurovascular regulation typical of arteriolar vessels, some pharmacological agents which can preferentially create vasodilation in the skin or in normal organs have been observed to create conditions resulting in diversion of blood from the tumor to surrounding tissue, or “vascular steal” (41) (reviewed in Jirtle.(42)) and a reduction of IFP (43). We did not observe a reduction in tumor vascular flow in our study. This may be because thermoregulatory signals, unlike vessel dilating drugs (e.g., hydralazine or bradykinin), used for studies on vascular steal (44), result in compensatory vascular events, including constriction of blood vessels in the core organs, in order to maintain blood pressure and optimize delivery of heated blood to the skin. However, it is important to note that in our experiments, at least 1 hour passed before we tested blood flow in tumors following heating. It is possible that during the heating there may have been transient diversion of blood from the tumor, resulting in reduced IFP which in turn, ultimately resulted in increased tumor perfusion.

Clinical investigators working in the field of hyperthermic oncology often employ short-term local heating of tumors, usually from an external radiofrequency or ultrasound source, as an adjuvant for cancer therapy (21) and whether IFP is affected by this protocol in

patients has not been tested. When we used a local hyperthermia protocol in mice, we did not observe any changes in tumor IFP (unpublished observations) a result which is similar to that reported earlier by others (45). However, in comparing the outcomes of different heating protocols in terms of effects on vasomotor parameters and IFP, it may be very important to consider the heating source, the duration of heating and temperature achieved and whether general anesthetics are used. A report by Leunig et al., (46) using local hyperthermia at 43°C reported a reduction in tumor IFP; however, in that study, the cytotoxic temperature resulted in vascular collapse through rapid endothelial cell death. Further, unlike the protocol used here in which the animals are not restrained or anesthetized, most local hyperthermia experiments on mouse and rat models employ a general anesthetic (e.g. ketamine mixtures) to subdue the animal. Since general anesthetics such as ketamine are known to cause vasoconstriction (47), it is likely that the thermoregulatory responses (and subsequent changes in IFP and vascular perfusion) may be limited.

Whole body hyperthermia on tumor bearing rat and mouse models has also been performed (28, 29, 33) as well as whole body heating in patients (48); however, tumor IFP was not measured in those studies. A recent Phase III clinical trial in which patients with high-risk sarcoma (49) were treated with “deep regional” hyperthermia in combination with chemoradiotherapy revealed significant positive benefits. This regional heating protocol, which heats larger volumes of tissue in comparison to local hyperthermia, may also engage thermoregulatory responses. However, measurements of IFP or intratumoral vascular perfusion were not conducted in this trial. Acquiring this information will be an exciting opportunity to understand better the clinical benefits that can be achieved with various hyperthermia protocols.

In summary, we show here that mild warming of mice results in non-cytotoxic, highly physiologically relevant changes in the tumor microenvironment, providing a potential window of time in which improved vascular access to the tumor can be achieved for therapy. Exploiting thermoregulation has the attractive feature of being more universally applicable than many other approaches, and could be more easily combined with other therapies, reducing exposure to cytotoxic drugs. An intriguing possibility is that sustained exercise, known to stimulate many of the same thermoregulatory responses as increased ambient temperature, (31, 50) may also have a positive effect on reducing tumor IFP. Collectively, these results provide a strong rationale for exploiting normal thermoregulatory responses to improve efficacy of therapies that are dependent on vascular perfusion and compromised by high intratumoral pressures.

Acknowledgments

This research was supported by grants from the NCI (CA135368, CA94045, and CA 071599). The authors thank Drs. Christopher Gordon and John Subjeck for their advice on the manuscript and data, and also Jeanne Prendergast for her help with nearly all aspects of this research.

Bibliography and References Cited

1. Jain RK. Barriers to drug delivery in solid tumors. Sci Am. 1994; 271(1):58–65. [PubMed: 8066425]
2. Dvorak HF. How Tumors Make Bad Blood Vessels and Stroma. Am J Pathol. 2003; 162(6):1747–57. [PubMed: 12759232]
3. Vaupel P. Tumor microenvironmental physiology and its implications for radiation oncology. Semin Radiat Oncol. 2004; 14(3):198–206. [PubMed: 15254862]
4. Stohrer M, Boucher Y, Stangassinger M, Jain RK. Oncotic pressure in solid tumors is elevated. Cancer Res. 2000; 60(15):4251–5. [PubMed: 10945638]

5. Heldin CH, Rubin K, Pietras K, Ostman A. High interstitial fluid pressure - An obstacle in cancer therapy. Nature Reviews Cancer. 2004; 4(10):806–13.
6. Fukumura D, Jain RK. Tumor microvasculature and microenvironment: targets for anti-angiogenesis and normalization. Microvasc Res. 2007; 74(2–3):72–84. [PubMed: 17560615]
7. Roh HD, Boucher Y, Kalnicki S, Bauchsbaum R, Bloomer WD, Jain RK. Interstitial hypertension in carcinoma of uterine cervix in patients: Possible correlation with tumor oxygenation and radiation response. Cancer Research. 1991; 51:6695–8. [PubMed: 1742744]
8. Milosevic MMD, Fyles AMD, Hill RPP. Interstitial Fluid Pressure in Cervical Cancer: Guide to Targeted Therapy. American Journal of Clinical Oncology. 2001; 24(5):516–21. [PubMed: 11586107]
9. Lunt SJ, Kalliomaki TMK, Brown A, Yang VX, Milosevic M, Hill RP. Interstitial fluid pressure, vascularity and metastasis in ectopic, orthotopic and spontaneous tumours. BMC Cancer. 2008; 8
10. Griffon-Etienne G, Boucher Y, Brekken C, Suit HD, Jain RK. Taxane-induced apoptosis decompresses blood vessels and lowers interstitial fluid pressure in solid tumors: clinical implications. Cancer Res. 1999; 59(15):3776–82. [PubMed: 10446995]
11. Ozerdem U, Hargens AR. A simple method for measuring interstitial fluid pressure in cancer tissues. Microvascular Research. 2005; 70(1–2):116–20. [PubMed: 16137719]
12. Ferretti S, Allegrini PR, Becquet MM, McSheehy PMJ. Tumor interstitial fluid pressure as an early-response marker for anticancer therapeutics. Neoplasia. 2009; 11(9):874–81. [PubMed: 19724681]
13. Jain RK. Transport of molecules across tumor vasculature. Cancer and Metastasis Review. 1987; 6(4):559–93.
14. Minchinton AI, Tannock IF. Drug penetration in solid tumours. Nature Reviews Cancer. 2006; 6(8):583–92.
15. Padera T, BR S, Tooredman JB, D. C, E. dT, RK J. Cancer cells compress intratumor vessels. Nature. 2004; 427:695. [PubMed: 14973470]
16. Taghian AG, Abi-Raad R, Assaad SI, et al. Paclitaxel decreases the interstitial fluid pressure and improves oxygenation in breast cancers in patients treated with neoadjuvant chemotherapy: Clinical implications. Journal of Clinical Oncology. 2005; 23(9):1951–61. [PubMed: 15774788]
17. Lee CG, Heijn M, Di Tomaso E, et al. Anti-vascular endothelial growth factor treatment augments tumor radiation response under normoxic or hypoxic conditions. Cancer Research. 2000; 60(19): 5565–70. [PubMed: 11034104]
18. Moeller BJ, Richardson RA, Dewhirst MW. Hypoxia and radiotherapy: opportunities for improved outcomes in cancer treatment. Cancer Metastasis Rev. 2007; 26(2):241–8. [PubMed: 17440683]
19. Cerniglia GJ, Pore N, Tsai JH, et al. Epidermal growth factor receptor inhibition modulates the microenvironment by vascular normalization to improve chemotherapy and radiotherapy efficacy. PLoS ONE. 2009; 4(8)
20. Rofstad EK, Ruud EBM, Mathiesen B, Galappathi K. Associations between radiocurability and interstitial fluid pressure in human tumor xenografts without hypoxic tissue. Clinical Cancer Research. 2010; 16(3):936–45. [PubMed: 20103667]
21. Vigilianti, BL.; Stauffer, P.; Repasky, E.; Jones, E.; Dewhirst, M. Hyperthermia. In: Hong, W.; Blast, R., Jr; Hait, W., et al., editors. Holland-Frei Cancer Medicine. 8 ed. People's Medical Publishing House; USA: 2010.
22. Corry PM, Dewhirst MW. Thermal medicine, heat shock proteins and cancer. International Journal of Hyperthermia. 2005; 21(8):675–7. [PubMed: 16338847]
23. Roti Roti JL. Cellular responses to hyperthermia (40–46Â°C): Cell killing and molecular events. International Journal of Hyperthermia. 2008; 24(1):3–15. [PubMed: 18214765]
24. Griffin RJ, Dings RPM, Jamshidi-Parsian A, Song CW. Mild temperature hyperthermia and radiation therapy: Role of tumour vascular thermotolerance and relevant physiological factors. International Journal of Hyperthermia. 2010; 26(3):256–63. [PubMed: 20210610]
25. Vaupel PW, Kelleher DK. Pathophysiological and vascular characteristics of tumours and their importance for hyperthermia: Heterogeneity is the key issue. International Journal of Hyperthermia. 2010; 26(3):211–23. [PubMed: 20345270]

26. Song CW, Park H, Griffin RJ. Improvement of tumor oxygenation by mild hyperthermia. Radiation Research. 2001; 155(4):515–28. [PubMed: 11260653]
27. Vujaskovic Z, Song CW. Physiological mechanisms underlying heat-induced radiosensitization. International Journal of Hyperthermia. 2004; 20(2):163–74. [PubMed: 15195511]
28. Sakaguchi Y, Makino M, Kaneko T, et al. Therapeutic efficacy of long duration-low temperature whole body hyperthermia when combined with tumor necrosis factor and carboplatin in rats. Cancer Research. 1994; 54(8):2223–7. [PubMed: 8174130]
29. Sakaguchi Y, Stephens LC, Makino M, et al. Apoptosis in tumors and normal tissues induced by whole body hyperthermia in rats. Cancer Research. 1995; 55(22):5459–64. [PubMed: 7585616]
30. Xu Y, Choi J, Hylander B, et al. Fever-range whole body hyperthermia increases the number of perfused tumor blood vessels and therapeutic efficacy of liposomally encapsulated doxorubicin. International Journal of Hyperthermia. 2007; 23(6):513–27. [PubMed: 17952765]
31. Guyton, A.; Hall, J. Text Book of Medical Physiology. 11 ed.. Elsevier, Inc.; Philadelphia, PA: 2006. Body temprature, temperature regulation and fever. Chapter 73; p. 889-900.
32. Gordon, C. Temperature regulation in laboratory rodents. Cambridge Univ. Press; New York, NY: 1993. Thermoregulatory effector responses and Body temperature Chapters 4 and 5; p. 73-134.
33. Burd R, Dziedzic TS, Xu Y, Caligiuri MA, Subjeck JR, Repasky EA. Tumor cell apoptosis, lymphocyte recruitment and tumor vascular changes are induced by low temperature, long duration (fever-like) whole body hyperthermia. Journal of Cellular Physiology. 1998; 177(1):137–47. [PubMed: 9731754]
34. Trotter MJCD, Olive PL. Use of a carbocyanine dye as a marker of functional vasculature in murine tumours. British Journal of Cancer. 1989; 59:706–9. [PubMed: 2472164]
35. Bhujwalla ZM, Artemov D, Natarajan K, Solaiyappan M, Kollars P, Kristjansen PEG. Reduction of Vascular and Permeable Regions in Solid Tumors Detected by Macromolecular Contrast Magnetic Resonance Imaging after Treatment with Antiangiogenic Agent TNP-470. Clin Cancer Res. 2003; 9(1):355–62. [PubMed: 12538488]
36. Schmiedl U, Ogan M, Paajanen H. Albumin labeled with Gd-DTPA as an intravascular, blood pool-enhancing agent for MR imaging: Biodistribution and imaging studies. Radiology. 1987; 162(1):205–10. [PubMed: 3786763]
37. Bhattacharya A, Toth K, Mazurchuk R, et al. Lack of microvessels in well-differentiated regions of human head and neck squamous cell carcinoma A253 associated with functional magnetic resonance imaging detectable hypoxia, limited drug delivery, and resistance to irinotecan therapy. Clinical Cancer Research. 2004; 10(23):8005–17. [PubMed: 15585636]
38. Gordon C. Influence of heating rate on control of heat loss from the tail in mice. Am J Physiol. 1983; 244:R778–84. [PubMed: 6859290]
39. Gordon C. Behavioral and autonomic thermoregulation in mice exposed to microwave radiation. J Appl Physiol. 1983; 55:1242–8. [PubMed: 6629957]
40. Charkoudian N. Skin blood flow in adult human thermoregulation: How it works, when it does not, and why. Mayo Clinic Proceedings. 2003; 78(5):603–12. [PubMed: 12744548]
41. von Ardenne M. Synergic therapeutic effect of selective local hyperthermia and selective optimized hyperacidity against tumors. Theoretical and experimental bases. Ther Ggw. 1977; 166:1299–316.
42. Jirtle R. Chemical modification of tumor blood flow. Int J Hyperthermia. 1988; 4:356–72.
43. Zlotecki RA, Baxter LT, Boucher Y, Jain RK. Pharmacologic modification of tumor blood flow and interstitial fluid pressure in a human tumor xenograft: Network analysis and mechanistic interpretation. Microvascular Research. 1995; 50(3):429–43. [PubMed: 8583955]
44. Dewhirst MW, Vinuya RZ, Ong ET, et al. Effects of bradykinin on the hemodynamics of tumor and granulating normal tissue microvasculature. Radiation Research. 1992; 130(3):345–54. [PubMed: 1594761]
45. Hauck ML, Coffin DO, Dodge RK, Dewhirst MW, Mitchell JB, Zalusky MR. A local hyperthermia treatment which enhances antibody uptake in a glioma xenograft does not affect tumor interstitial fluid pressure. Int J Hyperthermia. 1997; 13(3):307–16. [PubMed: 9222813]
46. Leunig, M.; Goetz, AE.; Dellian, M., et al. Interstitial Fluid Pressure in Solid Tumors following Hyperthermia: Possible Correlation with Therapeutic Response. 1992. p. 487-90.

47. Brookes ZLS, Brown NJ, Reilly CS. Intravenous anaesthesia and the rat microcirculation: The dorsal microcirculatory chamber. British Journal of Anaesthesia. 2000; 85(6):901–3. [PubMed: 11732528]

48. Bull JMC, Scott GL, Strebel FR, et al. Fever-range whole-body thermal therapy combined with cisplatin, gemcitabine, and daily interferon-Î±: A description of a phase I-II protocol. International Journal of Hyperthermia. 2008; 24(8):649–62. [PubMed: 18608594]

49. Issels RD, Lindner LH, Verweij J, et al. Neo-adjuvant chemotherapy alone or with regional hyperthermia for localised high-risk soft-tissue sarcoma: A randomised phase 3 multicentre study. The Lancet Oncology. 2010; 11(6):561–70. [PubMed: 20434400]

50. McArdle, W.; Katch, F.; Katch, V. Excercise Physiology. 7th ed.. Wolters Kluwer; Lippincott Williams & Wilkins; New York, NY: 2010. Excercise and Thermal Stress, Chapter 25; p. 611-38.

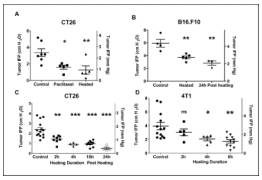

Figure 1. An increase in core body temperature decreases tumor interstitial fluid pressures in syngeneic tumors in BALB/c (CT26 and 4T1) and in C57BL/6 (B16.F10) mice

Heated mice bearing tumors (300–600mm^3) were maintained at 39.5°C for indicated time, returned to room temperature for 2 hours and then IFP measurements were performed. Each data point represents the average of multiple measurements in a single tumor. (A) CT26 tumors implanted subcutaneously on the hind leg: IFP of tumors in control untreated mice compared to IFP of tumors in mice treated with either 2 doses of paclitaxel (30mg/kg) or heat treatment. (B) B16.F10 tumors implanted subcutaneously on the flank: IFP of tumors in control untreated mice compared to IFP of tumors in mice heated to 39.5°C for 6h. (C) CT26 tumors implanted subcutaneously on the hind leg: IFP of tumors in control mice compared to IFP of tumors in mice after 2h or 4 h heating and 18h and 24h after a 6h heating. (D) 4T1 tumors implanted orthotopically in the 4th mammary fat pad. (300–600mm^3). IFP of tumors in control mice and of tumors in mice following 2h, 4h or 6h heating. IFP measurements are given in both cm H_2O and mm Hg. ANOVA with Dunnett's multiple comparison was used to test for statistical difference between the mean of the control group and the means of the treated groups (* p,0.05; ** p<0.01; *** p<0.001)

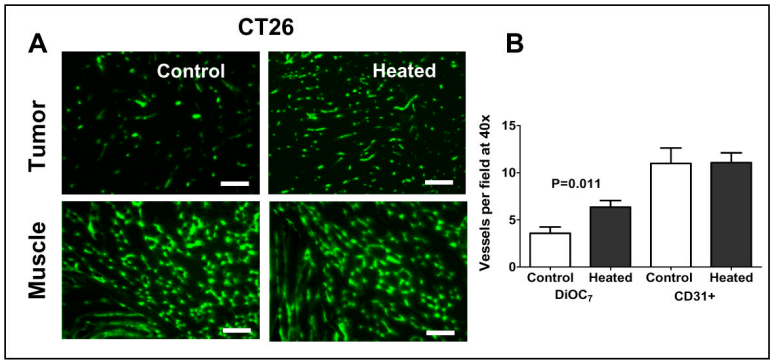

Figure 2. Elevated body temperature increases tumor blood vessel perfusion in BALB/c mice bearing CT26 tumors

(A) Representative fluorescence micrographs of CT26 tumor implanted subcutaneously on the hind leg (300–600mm^3 in volume, upper pair) and muscle (lower pair) showing perfused blood vessels following tail vein injection of the cyanine dye $DiOC_7(3)$. The micrographs on the left are those obtained from tissue excised from unheated control mice and the two on the right are from mice after 6h heating. The increased number of perfused vessels in a tumor from a heated mouse (160 vessels/this field) is apparent in comparison to that of an untreated mouse (82 vessels/this field). There is no visible difference in the number of perfused vessels in muscles from unheated control and that from heated animals. (B) The average total number of perfused, $DiOC_7(3)$ labeled blood vessels in tumors from untheated control mice and those from heated mice showing a doubling in the number of perfused vessels. The average numbers of anatomical CD31+ vessels are not altered by heating. Scale bars represent 500 μm.

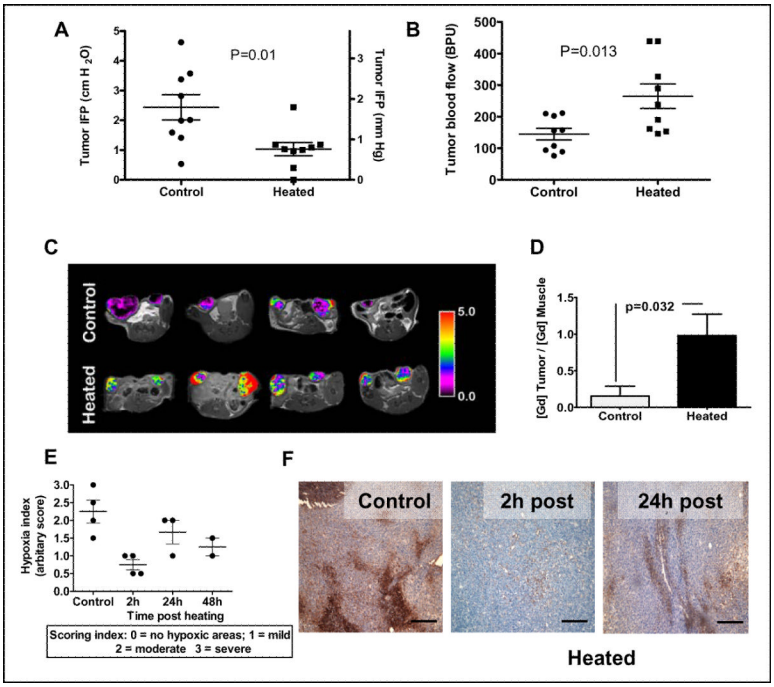

Figure 3. Thermally-induced increases in tumor blood flow correlate with decreases in tumor IFP and tissue hypoxia in CT26 tumors

(A) IFP and (B) blood flow changes (as measured by laser Doppler) following heating (n=9/group) of BALB/c mice bearing CT26 tumors implanted subcutaneously on the flanks (300–600mm^3 in volume). In these mice, blood flow was measured first and then IFP measurements were taken. (C) Changes in blood flow in CT26 tumors implanted subcutaneously on the hind legs (200–400mm^3 in volume) following heating documented by MRI: Representative pseudo-colorized images of contrast agent enhancement in four control animals (top) and another four animals following heating (bottom). Tumors in heated animals consistently showed higher amounts of the contrast agent than tumors in control animals, indicating a higher fractional volume of functioning vasculature as a result of heating. Color scale reflects the ratio of the contrast agent in tumors to normal tissue (back muscle). (D) Plot of the normalized vascular volumes in tumors from unheated control mice and those that heated. Data presented represent the average of each group (control n=8, heated n=10). P-values are Students' T-test results between the control and treated data sets. (D) Plot of the normalized vascular volumes in tumors from unheated control mice and those that heated. Vascular volumes were determined using a macromolecular MR contrast agent HSA-Gd-DTPA. Data presented represent the average of each group (control n=8, heated n=10). P-values are Students' T-test results between the control and the treated data sets. (E) Scatter plot of hypoxia index in tumors (implanted subcutaneously on the flanks, 300–600mm^3 in volume) from untreated mice and treated mice at 2, 24 and 48h post heating. (F) Immunohistochemical localization of pimonidazole (Hypoxyprobe-1) adducts in tumors from control mice and from heated mice at 2h and 24h post-heating. A reduction in hypoxic areas in the tumor sections (brown staining) following heating can be seen. Scale bars represent 500 μm.

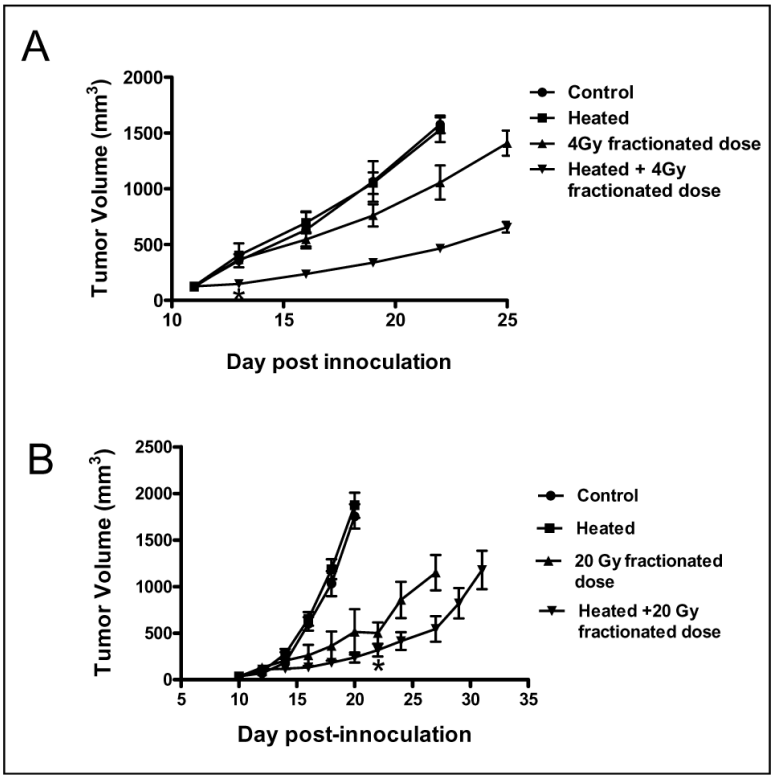

Figure 4. Heat treatment enhances the efficacy of radiation therapy in two different tumor models

(A) CT26 tumors were implanted subcutaneously on the flank of BALB/c mice. Tumor growth was then monitored in the following groups (n=5 per group): control untreated mice (●), mice that only heated (■), mice that received only radiation (1Gy daily for 4 days, days 12–15; ▲) and mice that heated and followed 24h later by four consecutive radiation treatments (1Gy daily for 4 days, days 12–15; ▼). Tumor growth rates in the unheated control and the heat-only groups were indistinguishable. The slowest growth rate was observed in tumors of mice that received the combination of heating followed by fractionated radiation. Statistical test using oneway ANOVA with Dunnett's multiple comparison tests for the means of the treated groups to the mean of the control group show significant difference only for the group of mice that received combined heating and radiation. (B) B16.F10 tumors were implanted subcutaneously on the flank of C57BL/6 mice. Kinetics of B16.F10 tumor growth in C57BL/6 mice (n=5), control untreated mice (●) and those that were only heated (day 10; ■), only radiation (days 11–15; ▲) and combined radiation and heating (▼). Tumor growth rates in the unheated control and the heating-only groups were comparable. The slowest growth rate was observed in tumors of mice that received fractionated 20Gy radiation (4Gy/day) starting one day after heating. Tumor volumes in the combined heat and radiation treatment group were significantly smaller ($P<0.05$) as compared to the radiation only group from day 24.